crystals

MDPI

Communication

The Anti-Reflection Coating Design for the Very-Long-Wave Infrared Si-Based Blocked Impurity Band Detectors

Zuoru Dong †, Yangzhou Zhou †, Yulu Chen *, Jiajia Tao, Wenhui Liu, Xiaowan Dai, Bingbing Wang, Yifei Wu and Xiaodong Wang *

Shanghai Microwave Technology Research Institute, Shanghai 200063, China
* Correspondence: chenyulu@50.sh.cn (Y.C.); nkwxd@mail.sitp.ac.cn (X.W.)
† These authors contributed equally to this work.

Abstract: An anti-reflection coating on a back-illuminated 128 × 128 array Si-based blocked impurity band (BIB) detector in a very-long-wave infrared range was designed in this work. The reflectance and transmittance spectra of ZnS films with different thicknesses on intrinsic Si substrates were studied with a FDTD simulation and experiment. Compared to bare Si substrate, the reflectance of Si coated with 1.5, 2.0, 2.5, and 3.0 μm thick ZnS significantly decreased, while the transmittance increased in the range of 10.0~25.0 μm band. The transmittance enhancement ratio reached approximately 32%, 32%, 28%, and 29%, respectively. It was evidenced that the enhanced transmission at a specific wavelength was caused by the effective interference cancellation effect. Then, a 2.0 μm thick ZnS thin film was deposited on the backside of the 128 × 128 array Si-based BIB detector. The spectral responsivity of the detector increased significantly. Additionally, the blackbody responsivity increased by approximately 36%, suggesting that the ZnS film is an ideal anti-reflection material for VLWIR detectors in the range of 10.0~25.0 μm band.

Keywords: anti-reflection coating; Si-based BIB detector; reflectance spectra; blackbody responsivity

Citation: Dong, Z.; Zhou, Y.; Chen, Y.; Tao, J.; Liu, W.; Dai, X.; Wang, B.; Wu, Y.; Wang, X. The Anti-Reflection Coating Design for the Very-Long-Wave Infrared Si-Based Blocked Impurity Band Detectors. *Crystals* **2023**, *13*, 60. https://doi.org/10.3390/cryst13010060

Academic Editor: Marco Bazzan

Received: 1 November 2022
Revised: 11 December 2022
Accepted: 20 December 2022
Published: 29 December 2022

1. Introduction

The Si-based block impurity band (BIB) detector is an optimized structure of extrinsic semiconductor photoconductive detector, which mainly include a heavily doped absorption layer and a thin high-purity blocking layer [1–4]. The basic operation principle of Si-based BIB detectors is that the carriers transfer from the impurity band to the conduction band in the absorbing layer under the illumination of infrared radiation, which induces a spectral response band in a very-long-wave infrared range (VLWIR) of 5–25 μm [5]. Moreover, the dark current of the device is suppressed by employing the high-purity blocking layer to block the impurity band conduction. The Si-based BIB detector has the advantages of a wide response spectrum, low dark current, strong radiation resistance, and array imaging. It has a wide range of application prospects in astronomical observation, atmospheric monitoring, and non-destructive testing [6–11].

However, due to the high refractive index of Si, of approximately 3.4, within the VLWIR, high Fresnel loss, also known as surface reflection loss, would occur at the Si–air interface [12,13]. It would limit the photon absorption efficiency of the detector and seriously reduce the detection efficiency of the device. Hence, it is necessary to use anti-reflection techniques. Various anti-reflection techniques have been studied, such as surface plasmons, meta-materials, and anti-reflection coatings [14–16]. Among them, anti-reflection coatings have attracted interest for use in a wide range of industries and applications due to their high surface hardness, excellent stability, and good attachability [17]. He et al. and Carrasco et al. used anti-reflection coatings, such as SiNx, to improve the detection efficiency of InGaAs detectors [18,19]. D'souza et al. and Saini et al. investigated YF_3 and ZnS double-layer and multi-layer anti-reflection coatings for HgCdTe detectors through the

use of theories and experiments, respectively [4,20]. De Vita et al. deposited a ZnS-based anti-reflection coating on a Si plate, after which a transmission enhancement ratio of 28% was obtained at the wavelength range of 6–14 μm [21]. Nevertheless, the research on anti-reflection coatings has mainly focused on infrared detectors with response wavelengths of less than 14 μm, while research on anti-reflection coatings applicable to Si-based BIB detectors with a response in the VLWIR range has rarely been reported yet. Therefore, the design and preparation of VLWIR anti-reflection coatings integrated with Si-based BIB detectors need to be fully investigated.

Among several available transparent materials in the VLWIR, such as ZnS, ZnSe, MgF_2, diamond, etc., ZnS is non-toxic, non-hygroscopic, and compatible with Si processes, which can be deposited throughout the use of sputtering and evaporation at room temperature [22,23]. Moreover, its refractive index (approximately 1.9) is close to the square root of the refractive index of Si (approximately 3.4), satisfying the single anti-reflection coating's reflectivity equation [24]. Thus, the reflectance and transmittance characteristics of the ZnS thin film on an intrinsic Si substrate were studied with a finite difference time domain (FDTD) simulation and experiment. Compared to bare Si substrate, the reflectance of the ZnS/Si structures in the range of 10.0~25.0 μm band reduced significantly, and the transmittance obviously increased, based on the interference effect of the film. Finally, by depositing a 2.0 μm ZnS film on the backside of the 128 × 128 array Si-based BIB detector, the spectral responsivity of the detector increased significantly, and blackbody responsivity increased by approximately 36%.

2. Materials and Methods

To study the anti-reflection characteristics of the ZnS intuitively, the reflectance and transmittance spectra of the ZnS films with different thicknesses on intrinsic Si substrates were investigated with a FDTD simulation and experiment. The FDTD model of the ZnS/Si structure is shown in Figure 1a. The thickness of the ZnS layer was successively set as 1.5, 2.0, 2.5, and 3.0 μm, and that of the Si substrate was set as 500 μm. The monitors for reflection and transmission records were placed above and below the ZnS/Si structure, respectively. The measured material parameters, such as the refractive indexes of Si and ZnS (shown in Figures S1 and S2 in the Supplementary Materials), were used in the simulation. Additionally, the boundary conditions were periodic.

Then, ZnS films with a thickness of approximately 1.5, 2.0, 2.5, and 3.0 μm were deposited on Si substrates through electron beam evaporation at room temperature, respectively. During the deposition process, the background vacuum was better than 9×10^{-4} Pa and the deposition rate was maintained at 1.5 Å/s. The reflectance and transmittance spectra of the ZnS/Si structures were measured at 4 K with a Bruker VERTEX 80 V Fourier transform infrared (FTIR) spectrometer.

Lastly, the Si-based BIB detector integrated with a ZnS coating was fabricated. The Si-based BIB detector was a 128 × 128 array with a pixel pitch of 45 μm, and was designed as a back-illuminated structure, as shown in Figure 1b. On the surface of the 500 μm thick intrinsic Si substrate, a B-doped negative electrode contact layer was fabricated through ion implantation and rapid thermal annealing. A P-doped absorbing layer with a concentration ratio of approximately 8×10^{17} cm^{-3} and an intrinsic block layer were deposited successively using chemical vapor deposition. Then, a B-doped positive electrode contact layer was formed. A V-groove was dug in the negative area to expose the electrode contact layer. Subsequently, the Ti/Al/Ni/Au electrode upon the contact layer was deposited through magnetron sputtering. The pixels were then electrically separated from each other with 15 μm wide and 20 μm deep grid-shaped ditches. At last, the ZnS coating with a thickness of 2.0 μm was deposited on the backside of the polished intrinsic Si substrate of the BIB detector using electron beam evaporation. Figure 1c shows the optical micrograph of the BIB detector with a pixel array of 128 × 128 and a pixel pitch of approximately 45 μm. The prepared detectors were packaged on the designed circuit substrate with the flip-chip method, as shown in Figure 1d. Then, the spectral response of the Si-based BIB detector was

measured at 4 K with a FTIR spectrometer. The blackbody responsivities of the BIB detector with and without the ZnS film were measured at 4 K using a 500 K blackbody source.

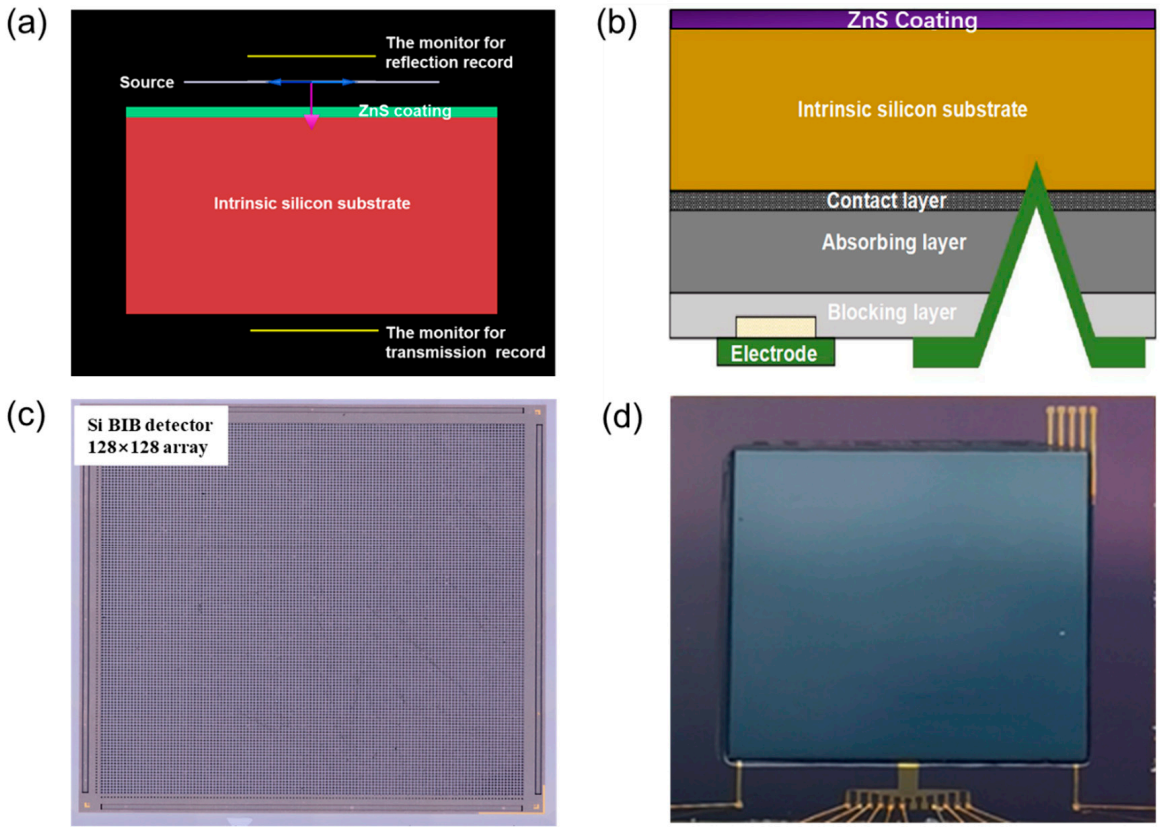

Figure 1. (**a**) Schematic diagram of ZnS/Si model. (**b**) The structure of the back-illuminated Si-based BIB detector integrated with ZnS coating. (**c**) Optical micrograph of the Si-based BIB detector. (**d**) Photo image of the packaged BIB detector.

3. Results

Figure 2a,b show the reflectance and transmittance spectra of the ZnS/Si structure simulated using FDTD, where the thickness of the ZnS layer varied. It was found that the reflectance of the bare Si substrate was approximately 30% in the range of 10.0~25.0 μm due to the mismatch of refractive indices between the Si and the air, while the reflectance of the Si coated with ZnS significantly decreased and transmittance increased. As for the Si coated with 1.5, 2.0, 2.5, and 3.0 μm thick ZnS layers, the reflectance of the ZnS/Si structure could be significantly reduced by up to 2.0%, 1.0%, 0.3%, and 0.4%, and the transmittance could be increased up to 97%, 97%, 96%, and 93%, respectively. The corresponding transmittance enhancement ratios were approximately 39%, 39%, 37%, and 33%. This demonstrated that the ZnS film was an ideal anti-reflection coating in the VLWIR band. Meanwhile, with the thickness of the ZnS coating increasing, the minimum valley positions of the reflectance spectra and the peak positions of the transmittance spectra red shifted from 13.4 to 17.2, 19.0, and 22.0 μm. This was highly consistent with the interference cancellation formula [24],

$$d = \lambda/4n_1,$$

where d is the thickness of the ZnS, λ is the wavelength of the incident light, n_1 is the refractive index of the ZnS, and the value of n_1 is approximately 1.9. This suggests that the reduction in reflectance for the ZnS/Si structure was caused by the effective interference cancellation effect.

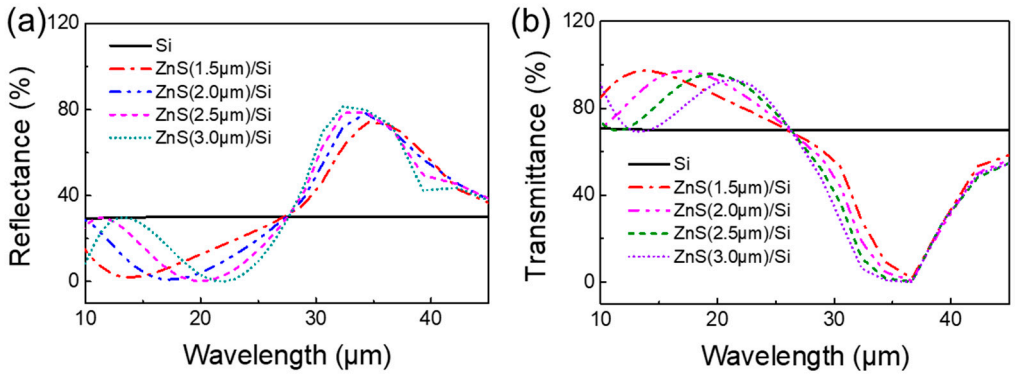

Figure 2. (**a**) Reflectance and (**b**) transmittance spectra of the Si and ZnS/Si structures simulated with FDTD, in which the thickness of the ZnS layer was set to 1.5, 2.0, 2.5, and 3.0 μm, respectively.

The reflectance and transmittance spectra of the ZnS/Si structures obtained in the experiment are shown in Figure 3a,b. It was observed that a reflection of approximately 45% was produced on the surface of the bare Si substrate. Such a large reflection would seriously affect the properties of corresponding devices. Compared to the bare Si substrate, the reflectance of the ZnS/Si structures in the range of 10.0~25.0 μm band significantly reduced, and the transmittance clearly increased. After successively depositing the 1.5, 2.0, 2.5, and 3.0 μm thick ZnS films on the polished silicon substrates, the minimum valley of the reflectance spectrum reduced to 24.5%, 23.9%, 14.6%, and 21.2%, and the corresponding transmittance increased to 70%, 66%, 62%, and 65%, respectively. The transmittance enhancement ratios reached approximately 32%, 32%, 28%, and 29%. Thus, it was concluded that the existence of the ZnS film could significantly reduce the reflectance and increase the absorptance of the device in the range of 10.0~25.0 μm band. Due to the manufacturing process deviation, the numerical values were smaller than the simulation results. Moreover, with the thickness of the ZnS film increasing, the minimum valley positions of the reflectance spectra and the maximum peak positions of the transmittance spectra red shifted from 11.7 to 20.4 μm. This correlated well with the FDTD simulation results.

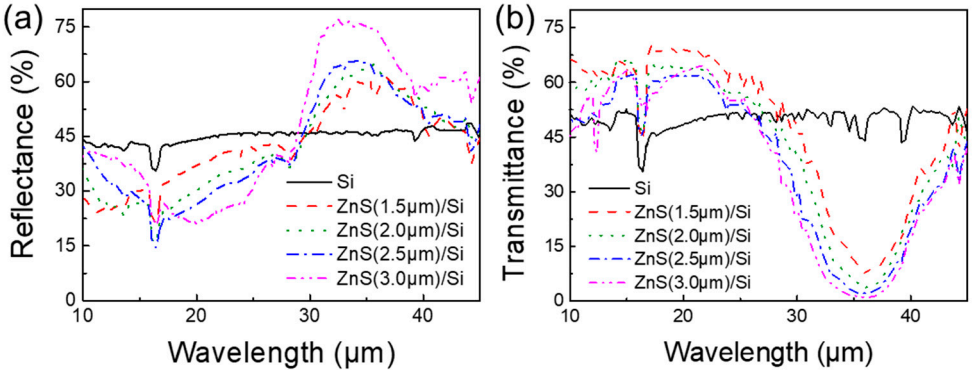

Figure 3. (**a**) Reflectance and (**b**) transmittance spectra of bare Si substrate and ZnS/Si structures, where the thicknesses of the ZnS layers were 1.5, 2.0, 2.5, and 3.0μm, respectively.

Since the response spectrum of the Si-based BIB detector was located at 17.0 μm, as shown in Figure 4a, it was in good agreement with the minimum peak position of the reflectance spectra of the ZnS (2.0 μm)/Si structure. Thus, a 2.0 μm thick ZnS film was deposited on the silicon-based BIB detector. The intensity of the spectral response peak for the ZnS (2.0 μm)/BIB detector was apparently stronger than that of the bare BIB detector. Then, the blackbody responsivities of the BIB detector before and after the ZnS film being deposited were detected. The data of three non-adjacent pixels were extracted, as shown in Figure 4b. Under 500 K blackbody radiation, the mean responsivity of the pixels with the 2.0 μm ZnS coating was approximately 1.01 A/W, while that of the pixels

without the ZnS coating was approximately 0.74 A/W at 2 V. Through calculations, the responsivity of the BIB detector was found to have increased significantly, by 36%, through being covered with a 2.0μm thick ZnS layer. This demonstrated that the ZnS coating would be an ideal anti-reflection coating for enhancing the performance of VLWIR Si-based BIB detectors. Additionally, the almost coincident blackbody responsivity curves showed that the anti-reflection film had good uniformity.

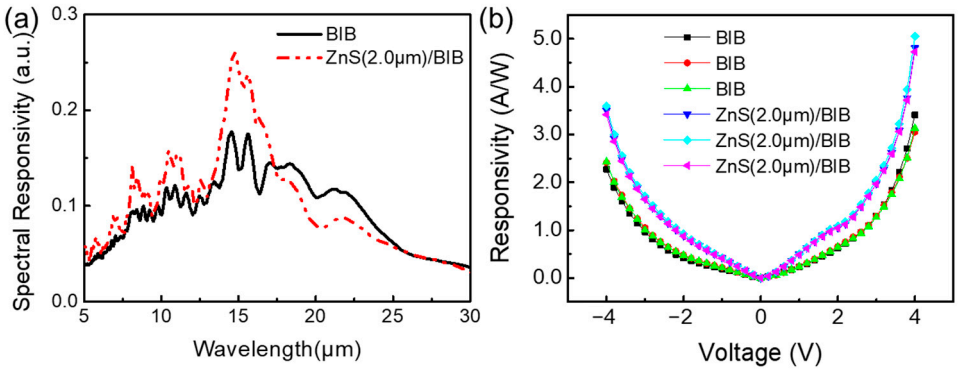

Figure 4. (**a**) Spectral responsivities of the Si-based BIB detector with and without ZnS coating. (**b**) Blackbody responsivity curves for three pixels of Si-based BIB detector with and without ZnS coating.

4. Conclusions

In this work, the reflectance and transmittance spectra of ZnS anti-reflection films with different thicknesses on intrinsic Si substrates were investigated with a FDTD simulation and experiment. Compared with bare Si substrate, the reflectance of the ZnS/Si structures significantly reduced, and the transmittance obviously increased in the range of 10.0~25.0 μm band. By depositing 1.5, 2.0, 2.5, and 3.0 μm ZnS successively onto Si substrates, transmittance enhancement ratios of approximately 32%, 32%, 28%, and 29% could be achieved. The redshifts of the reflectance and transmittance spectra peaks were consistent with the interference cancellation formula, indicating that the anti-reflection effect of the ZnS was caused by an interference cancellation. Finally, a 2.0 μm ZnS film was deposited on a 128 × 128 array BIB detector, resulting in a 36% increase in blackbody responsivity. This work provided an effective way to improve the performance of detectors in the VLWIR band.

Supplementary Materials: The following supporting information can be downloaded at: https://www.mdpi.com/article/10.3390/cryst13010060/s1, Figure S1: the complex refractive indexes of Si, Figure S2: the complex refractive indexes of ZnS.

Author Contributions: Conceptualization, Z.D. and Y.C.; methodology, Z.D. and Y.Z.; software, Y.Z.; validation, Z.D. and X.D.; formal analysis, Y.Z. and Y.W.; investigation, Z.D., J.T., W.L. and B.W.; resources, X.D.; data curation, Z.D., Y.W., W.L. and B.W.; writing—original draft preparation, Z.D. and Y.Z.; writing—review and editing, Y.C. and J.T.; visualization, Z.D. and Y.Z.; supervision, Y.C. and X.W.; project administration, Y.C. and X.W.; funding acquisition, Y.C. and X.W. All authors have read and agreed to the published version of the manuscript.

Funding: This research was funded by the National Key R&D Program of China (no. 2021YFB2800700), the National Natural Science Foundation of China (grant no. 62171286), the Shanghai Outstanding Academic Leaders Plan (21XD1423600), and the Shanghai Youth-Notch Talent Development Program.

Data Availability Statement: The data that support the findings of this study are available from the corresponding authors upon reasonable request.

Conflicts of Interest: The authors declare no conflict of interest.

References

1. Haegel, N.M.; Jacobs, J.E.; White, A.M. Modeling of steady-state field distributions in blocked impurity band detectors. *Appl. Phys. Lett.* **2000**, *77*, 4389–4391. [CrossRef]
2. Stetson, S.; Reynolds, D.; Stapelbroek, M.; Stermer, R. Design and Performance of Blocked-Impurity-Band Detector Focal Plane Arrays. *Proc. SPIE Int. Soc. Opt. Eng.* **1985**, *686*, 48–65. [CrossRef]
3. Szmulowicz, F.; Madarsz, F.L. Blocked Impurity Band Detectors—An Analytical Model—Figures of Merit. *J. Appl. Phys.* **1987**, *62*, 2533–2540. [CrossRef]
4. Saini, A.K.; Singh, A.; Meena, V.S.; Kumar Gaur, S.; Pal, R. Design and development of double-layer anti-reflection coating for HgCdTe based mid-wave infrared detector. *Mater. Sci. Semicond. Process.* **2022**, *147*, 106749. [CrossRef]
5. Tschanz, S.J.; Garcia, J.C.; Haegel, N.M. Modeling the alternate bias configuration and low temperature C-V profiling in blocked impurity band detectors. In *Infrared Spaceborne Remote Sensing 2005, Proceedings of the Optics and Photonics 2005, San Diego, CA, USA, 31 July–4 August 2005*; SPIE: San Diego, CA, USA, 2005; pp. 172–183.
6. Rauter, P.; Fromherz, T.; Winnerl, S.; Zier, M.; Kolitsch, A.; Helm, M.; Bauer, G. Terahertz Si:B blocked-impurity-band detectors defined by nonepitaxial methods. *Appl. Phys. Lett.* **2008**, *93*, 261104. [CrossRef]
7. Garcia, J.C.; Haegel, N.M.; Zagorski, E.A. Alternate operating mode for long wavelength blocked impurity band detectors. *Appl. Phys. Lett.* **2005**, *87*, 043502. [CrossRef]
8. Wang, X.; Wang, B.; Chen, X.; Chen, Y.; Hou, L.; Xie, W.; Pan, M. Roles of blocking layer and anode bias in processes of impurity-band transition and transport for GaAs-based blocked-impurity-band detectors. *Infrared Phys. Technol.* **2016**, *79*, 165–170. [CrossRef]
9. Haegel, N.M. BIB detector development for the far infrared: From Ge to GaAs. In Proceedings of the Integrated Optoelectronics Devices, San Jose, CA, USA, 25–31 January 2003; Volume 4999.
10. Wright, E.L.; Eisenhardt, P.R.M.; Mainzer, A.K.; Ressler, M.E.; Cutri, R.M.; Jarrett, T.; Kirkpatrick, J.D.; Padgett, D.; McMillan, R.S.; Skrutskie, M.; et al. The Wide-Field Infrared Survey Explorer (Wise): Mission Description and Initial On-Orbit Performance. *Astron. J.* **2010**, *140*, 1868. [CrossRef]
11. Werner, M.W.; Roellig, T.L.; Low, F.J.; Rieke, G.H.; Rieke, M.; Hoffmann, W.F.; Young, E.; Houck, J.R.; Brandl, B.; Fazio, G.G.; et al. The Spitzer Space Telescope Mission. *Astrophys. J. Suppl. Ser.* **2004**, *154*, 1. [CrossRef]
12. Palik, E.D. *Handbook of Optical Constants of Solids II*; Academic Press Handbook Series; Palik, E.D., Ed.; Academic Press: New York, NY, USA, 1991; Volume 2.
13. Min, H.; Jianxin, C.; Yi, Z.; Zhicheng, X.; Li, H. Light-harvesting for high quantum efficiency in InAs-based InAs/GaAsSb type-II superlattices long wavelength infrared photodetectors. *Appl. Phys. Lett.* **2019**, *114*, 141102.
14. Bhatt, M.; Nautiyal, B.B.; Bandyopadhyay, P.K. High efficiency antireflection coating in MWIR region (3.6–4.9μm) simultaneously effective for Germanium and Silicon optics. *Infrared Phys. Technol.* **2010**, *53*, 33–36. [CrossRef]
15. Kumar, A.R.; Zhang, Z.M.; Boychev, V.A.; Tanner, D.B.; Vale, L.R.; Rudman, D.A. Far-Infrared Transmittance and Reflectance of $YBa_2Cu_3O_{7-\delta}$ Films on Si Substrates. *J. Heat Transf.* **1999**, *121*, 844–851. [CrossRef]
16. Bushunov, A.A.; Tarabrin, M.K.; Lazarev, V.A. Review of Surface Modification Technologies for Mid-Infrared Antireflection Microstructures Fabrication. *Laser Photonics Rev.* **2021**, *15*, 2000202. [CrossRef]
17. Guo, S.; Yang, L.; Dai, B.; Geng, F.; Ralchenko, V.; Han, J.; Zhu, J. Past Achievements and Future Challenges in the Development of Infrared Antireflective and Protective Coatings. *Phys. Status Solidi A* **2020**, *217*, 2000149. [CrossRef]
18. Carrasco, R.A.; George, J.; Maestas, D.; Alsaad, Z.M.; Garnham, D.; Morath, C.P.; Duran, J.M.; Ariyawansa, G.; Webster, P.T. Proton irradiation effects on InGaAs/InAsSb mid-wave barrier infrared detectors. *J. Appl. Phys.* **2021**, *130*, 114501. [CrossRef]
19. He, T.; Yang, X.; Tang, Y.; Wang, R.; Liu, Y. High photon detection efficiency InGaAs/InP single photon avalanche diode at 250 K. *J. Semicond.* **2022**, *43*, 102301. [CrossRef]
20. D'Souza, A.I.; Robinson, E.; Wijewarnasuriya, P.S.; Stapelbroek, M.G. Spectral Response Model of Backside-Illuminated HgCdTe Detectors. *J. Electron. Mater.* **2011**, *40*, 1657–1662. [CrossRef]
21. De Vita, C.; Asa, M.; Urquia, M.A.; Castagna, M.E.; Somaschini, C.; Morichetti, F.; Melloni, A. ZnS antireflection coating for Silicon for MIR–LWIR applications. In Proceedings of the 2021 IEEE 17th International Conference on Group IV Photonics (GFP), Malaga, Spain, 7–10 December 2021; pp. 1–2.
22. Fei, L.; Hongfei, J.; Jinlong, Z.; Bin, Y.; Huasong, L.; Yiqin, J.; Zhanshan, W.; Xinbin, C. High performance ZnS antireflection sub-wavelength structures with HfO_2 protective film for infrared optical windows. *Opt. Express* **2021**, *29*, 31058–31067.
23. Yu, T.; Qin, Y.; Liu, D. The coatings for a solar-rejected window of the infrared horizon sensor. *Infrared Phys. Technol.* **2020**, *105*, 103214. [CrossRef]
24. Nguyen, J.; Yu, J.S.; Evans, A.; Slivken, S.; Razeghi, M. Optical coatings by ion-beam sputtering deposition for long-wave infrared quantum cascade lasers. *Appl. Phys. Lett.* **2006**, *89*, 111113. [CrossRef]